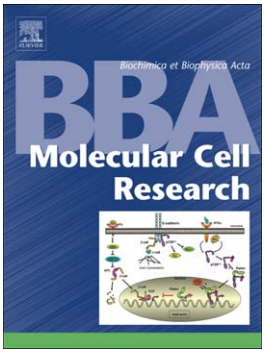

Resveratrol-induced autophagy is dependent on IP_3Rs and on cytosolic Ca^{2+}

Tomas Luyten, Kirsten Welkenhuyzen, Gemma Roest, Elzbieta Kania, Liwei Wang, Mart Bittremieux, David I. Yule, Jan B. Parys, Geert Bultynck

PII: S0167-4889(17)30047-2
DOI: doi:10.1016/j.bbamcr.2017.02.013
Reference: BBAMCR 18055

To appear in: *BBA - Molecular Cell Research*

Received date: 28 October 2016
Revised date: 22 February 2017
Accepted date: 25 February 2017

Please cite this article as: Tomas Luyten, Kirsten Welkenhuyzen, Gemma Roest, Elzbieta Kania, Liwei Wang, Mart Bittremieux, David I. Yule, Jan B. Parys, Geert Bultynck, Resveratrol-induced autophagy is dependent on IP_3Rs and on cytosolic Ca^{2+}, *BBA - Molecular Cell Research* (2017), doi:10.1016/j.bbamcr.2017.02.013

Resveratrol-induced autophagy is dependent on IP_3Rs and on cytosolic Ca^{2+}

Tomas LUYTEN[1,*], Kirsten WELKENHUYZEN[1,*], Gemma ROEST[1], Elzbieta KANIA[1], Liwei WANG[2], Mart BITTREMIEUX[1], David I. YULE[2], Jan B. PARYS[1,#], Geert BULTYNCK[1,#]

[1] KU Leuven, Laboratory of Molecular and Cellular Signaling, Department of Cellular and Molecular Medicine and Leuven Kanker Instituut, Campus Gasthuisberg O/N-I box 802, Herestraat 49, 3000 Leuven, Belgium

[2] University of Rochester, Department of Pharmacology and Physiology, Rochester, NY 14642, USA

* Shared first authors

[#] Shared senior co-authorship and correspondence:

Jan B. Parys and Geert Bultynck, Laboratory of Molecular and Cellular Signaling, KU Leuven Campus Gasthuisberg O/N-I box 802, Herestraat 49, 3000 Leuven, Belgium

JBP : Tel +32-16-330660 ; E-mail jan.parys@kuleuven.be

GB : Tel +32-16-330215 ; E-mail geert.bultynck@kuleuven.be

Disclosure statement: The authors declare no financial or other conflict of interest

Abstract

Previous work revealed that intracellular Ca^{2+} signals and the inositol 1,4,5-trisphosphate (IP_3) receptors (IP_3R) are essential to increase autophagic flux in response to mTOR inhibition, induced by either nutrient starvation or rapamycin treatment. Here, we investigated whether autophagy induced by resveratrol, a polyphenolic phytochemical reported to trigger autophagy in a non-canonical way, also requires IP_3Rs and Ca^{2+} signaling. Resveratrol augmented autophagic flux in a time-dependent manner in HeLa cells. Importantly, autophagy induced by resveratrol (80 µM, 2 h) was completely abolished in the presence of 10 µM BAPTA-AM, an intracellular Ca^{2+}-chelating agent. To elucidate the IP_3R's role in this process, we employed the recently established HEK 3KO cells lacking all three IP_3R isoforms. In contrast to the HEK293 wt cells and to HEK 3KO cells re-expressing IP_3R1, autophagic responses in HEK 3KO cells exposed to resveratrol were severely impaired. These altered autophagic responses could not be attributed to alterations in the mTOR/p70S6K pathway, since resveratrol-induced inhibition of S6 phosphorylation was not abrogated by chelating cytosolic Ca^{2+} or by knocking out IP_3Rs. Finally, we investigated whether resveratrol by itself induced Ca^{2+} release. In permeabilized HeLa cells, resveratrol neither affected the sarco- and endoplasmic reticulum Ca^{2+} ATPase (SERCA) activity nor the IP_3-induced Ca^{2+} release nor the basal Ca^{2+} leak from the ER. Also, prolonged (4 h) treatment with 100 µM resveratrol did not affect subsequent IP_3-induced Ca^{2+} release. However, in intact HeLa cells, although resveratrol did not elicit cytosolic Ca^{2+} signals by itself, it acutely decreased the ER Ca^{2+}-store content irrespective of the presence or absence of IP_3Rs, leading to a dampened agonist-induced Ca^{2+} signaling. In conclusion, these results reveal that IP_3Rs and cytosolic Ca^{2+} signaling are fundamentally important for driving autophagic flux, not only in response to mTOR inhibition but also in response to non-canonical autophagy inducers like resveratrol.

Keywords

cytosolic Ca^{2+}; inositol 1,4,5-trisphosphate; inositol 1,4,5-trisphosphate receptor; autophagy; resveratrol; HEK 3KO

Abbreviations

Akt, protein kinase B; AMPK, AMP-activated protein kinase; BAPTA-AM, 1,2-bis(o-aminophenoxy)ethane-N,N,N',N'-tetraacetic acid acetoxymethyl ester; DMEM, Dulbecco's modified Eagle's medium; EGTA, ethylene glycol tetraacetic acid; ER, endoplasmic reticulum; FCS, fetal calf serum; GAPDH, glyceraldehyde 3-phosphate dehydrogenase; IP_3, inositol 1,4,5-trisphosphate; IP_3R, inositol 1,4,5-trisphosphate receptor; JNK, c-Jun N-terminal kinase; LC3, microtubule-associated protein 1 light chain 3; mTOR, mechanistic target of rapamycin; p70S6K, 70 kDa S6 protein kinase; S6, S6 Ribosomal Protein; SERCA, sarco- and endoplasmic reticulum Ca^{2+} ATPase; STIM1, stromal interaction molecule 1; SOCE, store-operated calcium entry

1. Introduction

Macroautophagy, further referred to as autophagy, is a conserved degradation process by which bulk cytoplasm, long-lived proteins, organelles and intracellular pathogens are enclosed in double-membrane vesicles called autophagosomes and transported to the lysosomes for their eventual degradation [1]. Autophagy plays an important role in human health and disease as it helps to maintain nutrient and energy homeostasis, and to clear aggregated proteins, damaged organelles or infectious agents [2].

Ca^{2+} signaling has a complex impact on autophagy as depending on the cellular context, Ca^{2+} can stimulate or inhibit autophagy [3-6]. In particular, Ca^{2+} release from the endoplasmic reticulum (ER) was found to be required for the induction of autophagy in response to nutrient starvation [7, 8] and rapamycin [9]. Importantly, both starvation and rapamycin lead to inhibition of the mechanistic target of rapamycin (mTOR) and require Beclin 1 in the autophagy process. Yet, it is not known whether intracellular Ca^{2+} signaling is also involved in autophagy resulting from other mechanisms of induction.

Resveratrol (trans-3,4′,5-trihydroxystilbene), a polyphenol produced by many plant species has been reported to have several beneficial effects on health, including protection against cardiovascular problems [10, 11], neurodegeneration [12, 13] and cancer [14, 15]. As many other natural compounds, resveratrol is pleiotropic in its action [16] and affects proliferation, differentiation, apoptosis and autophagy [17]. The mechanisms by which resveratrol induces autophagy are still not completely elucidated. The first study reported that resveratrol induced autophagy via the NAD^+-dependent deacetylase sirtuin-1 [18, 19]. On the other hand, resveratrol can modulate starvation- and rapamycin-induced autophagy via the inhibition of the p70 S6 kinase (p70S6K) in a sirtuin-1 independent way [20]. Moreover, recent work indicated that resveratrol directly inhibits mTOR, which is located upstream of p70S6K, by binding to its ATP-binding site and thus competing with ATP for mTOR [21]. Resveratrol can also inhibit phosphoinositide 3-kinase upstream of protein kinase B (Akt) [22] and activate AMP-activated protein kinase (AMPK) both leading to mTOR inhibition [23, 24] and subsequent autophagy. Additionally, resveratrol can trigger autophagy by inducing c-Jun N-terminal kinase (JNK)-dependent accumulation of p62 [25]. Importantly, resveratrol-induced autophagy appears to occur via a non-canonical pathway as it is independent of Beclin 1 and of Vps34 [26, 27]. Since resveratrol induces autophagy by pathways that to a large part are different from those used by starvation or by

rapamycin, we decided to select this compound to induce autophagy and to assess the role of the IP_3R and of Ca^{2+} signaling.

Interestingly, resveratrol has been reported to directly provoke Ca^{2+} release in the cytosol by mobilizing Ca^{2+} from intracellular Ca^{2+} stores [28-30], though several observations are subject to caution as more recent work by us [31] and others [32, 33] have demonstrated an incompatibility between resveratrol and the use of the fluorescent Ca^{2+}-sensitive dye Fura-2.

Here, we have investigated the effect of resveratrol on autophagy in human cell lines including the recently developed HEK 3KO cells, in which the genes for all three inositol 1,4,5-trisphosphate (IP_3) receptor (IP_3R) isoforms have been disrupted by the CRISPR/Cas9 technique [34]. Our results indicate on the one hand that resveratrol acutely provokes Ca^{2+} leaking out of the ER via a mechanism that does not require IP_3Rs, thereby decreasing subsequent agonist-induced Ca^{2+} release, and on the other hand that its long-term autophagy-inducing properties critically depend on cytosolic Ca^{2+} signals and the presence of IP_3Rs.

2. Materials and Methods

2.1. Materials

Antibodies: mouse monoclonal anti-LC3 (1:500; nanoTools, 0231-100, Teningen, Germany); rabbit polyclonal anti-AMPKα (1:500; Cell Signaling Technology, 2532S, Danvers, MA, USA); rabbit monoclonal anti-phospho-AMPKα (Thr172) 40HG (1:500; Cell Signaling Technology, 2535S); rabbit polyclonal anti-Akt (1:500; Cell Signaling Technology, 9272S); rabbit polyclonal anti-phospho-Akt (Ser473) (1:500; Cell Signaling Technology, Cat. No. 9271S); rabbit monoclonal anti-S6 Ribosomal Protein 5G10 (1:500; Cell Signaling Technology, 2217S); rabbit monoclonal anti-phospho-S6 Ribosomal Protein (Ser235/236) D57.2.2E XP® (1:500; Cell Signaling Technology, 4858S); mouse monoclonal anti-glyceraldehyde 3-phosphate dehydrogenase (GAPDH, 1:50000; Sigma-Aldrich, G8795, St Louis, MO, USA); pan anti-IP_3R Rbt475 (1:1000) [35].

Reagents: resveratrol (Calbiochem, 554325, Darmstadt, Germany); 1,2-bis(o-aminophenoxy)ethane-N,N,N',N'-tetraacetic acid acetoxymethyl ester (BAPTA-AM; Invitrogen, Molecular Probes, B6769, Ghent, Belgium); Bafilomycin A1 (LC Laboratories, B-1080, Woburn, MA, USA); A23187 (Ascent Scientific Products, Asc-287, Cambridge, UK); ethylene glycol tetraacetic acid (EGTA; Acros Organics,

409910250, NJ, USA); ATP (Roche, 10127531001, Basel, Switzerland); $^{45}Ca^{2+}$ (PerkinElmer, NEZ013005MC, Waltham, MA, USA); thapsigargin (Alomone Labs, T-650, Jerusalem, Israel); IP_3 (Sigma-Aldrich, I-9766 or I7012) and Fluo-4-AM (Life Technologies, Ghent, Belgium).

2.2. Cell culture

Wild-type human cervix carcinoma cells (HeLa cells) were cultured at 37°C and 5% CO_2 in Dulbecco's modified Eagle's medium (DMEM) supplemented with 10% fetal calf serum (FCS) and 4 mM L-glutamine, 100 units/ml penicillin and 100 µg/ml streptomycin. HEK293 wild-type (HEK293 wt) and HEK 3KO cells were previously described [34]. HEK 3KO cells stably expressing rat IP_3R1 (HEK 3KO + IP_3R1) were generated by transfection of HEK 3KO cells with cDNA coding for rat IP_3R1 using the PolyJet™ *In Vitro* DNA Transfection Reagent (SignaGen Laboratories, Rockville, MD, USA) followed by two days of culture. HEK 3KO cells stably expressing IP_3R1 were selected by adding G418 (2 mg/ml) 48 hours after transfection. Serial cell dilution in 96-well plates was performed using G418-resistant cells to make single clones. HEK cells were cultured at 37°C and 10% CO_2 in DMEM supplemented with 10% FCS, 1% non-essential amino acids, 4 mM L-glutamine, 100 units/ml penicillin and 100 µg/ml streptomycin.

Both the HeLa and the HEK293 cell lines have been authenticated using autosomal STR profiling performed by the University of Arizona Genetics Core and fully matched the DNA fingerprint present in reference databases.

2.3. Western-blot analysis

Cells were scraped from the culture plate with ice-cold phosphate-buffered saline and lysed with RIPA buffer (20 mM Tris buffer pH 7.5, 10 mM sodium phosphate buffer, 150 mM NaCl, 1.5 mM $MgCl_2$, 0.5 mM dithiothreitol, 1% Triton X-100 and protease inhibitors) for 30 minutes at 4°C. The lysis solution was centrifuged and the supernatant was used for protein-concentration measurement. Protein samples (10 µg/lane) were separated on 4–12% Bis/Tris SDS–polyacrylamide gels, transferred to PVDF membranes (Thermo Scientific, Rockford, IL, USA) and blocked with phosphate-buffered saline containing 0.1% Tween-20 and 5% non-fat dry milk powder. The blocked membranes were incubated with the primary antibodies for 1 hour at room temperature or overnight at 4°C and after 3 wash steps subsequently incubated for 1 hour with secondary antibodies conjugated to horse radish peroxidase. Immunoreactive

proteins were visualized by using Pierce® ECL Western Blotting Substrate or Supersignal® West Dura Extended Duration Substrate (Thermo Scientific, Rockford, IL, USA). Protein bands were scanned using the ChemiDoc™ MP System (Bio-Rad, Nazareth Eke, Belgium), and quantified with Image Lab™ from Bio-Rad Laboratories.

2.4. Measurement of agonist- or thapsigargin-induced Ca^{2+} release in intact cells

HeLa cells were seeded ($6x10^4$ per well) in 96-well plates and after three days treated as indicated in the legends to the figures. For measuring the cytosolic [Ca^{2+}], the cell-culture medium was removed and the cells were washed once with modified Krebs solution (135 mM NaCl, 5.9 mM KCl, 1.2 mM $MgCl_2$, 11.6 mM HEPES, 11.5 mM glucose and 1.5 mM $CaCl_2$). Cells were loaded with Fluo-4-AM (2 µM) for 30 min at room temperature in modified Krebs solution. The cells were then washed with the same solution and incubated for 30 min in the absence of Fluo-4-AM. Forty seconds after addition of 3 mM EGTA, resveratrol or vehicle was added and 230 seconds later Ca^{2+} release was induced by the addition of either ATP (20 µM) or thapsigargin (2 µM). Fluorescence was subsequently measured with a FlexStation 3 benchtop multi-mode microplate reader (Molecular Devices, Sunnyvale, CA, USA) by exciting the dye at 488 nm while measuring the fluorescence emission at 530 nm.

2.5. Single-cell ER Ca^{2+} imaging

Single-cell ER Ca^{2+} measurements were performed as previously described [36, 37]. ER Ca^{2+} levels were measured with the genetically encoded Ca^{2+} indicator G-CEPIA1er, which was kindly provided by Dr. M. Iino (The University of Tokyo, Japan) [45]. The G-CEPIA1er construct was introduced into the HeLa and HEK cells utilizing X-tremeGENE HP DNA transfection reagent (Roche, Mannheim, Germany, 06366546001) according to the manufacturer's protocol. A Zeiss Axio Observer Z1 Inverted Microscope equipped with a 20x air objective and a high-speed digital camera (Axiocam Hsm, Zeiss, Jena, Germany) were used for these measurements. Changes in fluorescence were monitored in the GFP channel (480/520 nm excitation/emission). To chelate extracellular Ca^{2+}, 3 mM EGTA was added after 30 seconds. 40 seconds later resveratrol or DMSO as a control was added and 200 seconds later 2 µM thapsigargin was added. All traces were normalized (F/F0) where F0 is the starting fluorescence of each trace.

2.6. Unidirectional $^{45}Ca^{2+}$-flux assay

Unidirectional $^{45}Ca^{2+}$ flux assays were essentially performed as previously described [8, 38, 39]. In short, cells were permeabilized with saponin-containing permeabilization solution (120 mM KCl, 30 mM imidazole-HCl (pH 6.8), 2 mM $MgCl_2$, 1 mM K-EGTA, 1 mM Na-ATP, 20 µg/ml saponin) and were loaded with $^{45}Ca^{2+}$ in loading medium (120 mM KCl, 30 mM imidazole-HCl (pH 6.8), 5 mM $MgCl_2$, 0.44 mM K-EGTA, 5 mM Na-ATP, 10 mM NaN_3, and 150 nM free $^{40}CaCl_2$ + $^{45}CaCl_2$) for 45 min. After removal of the loading medium, the permeabilized cells were washed twice in efflux medium (120 mM KCl, 30 mM imidazole-HCl (pH 6.8) and 1 mM EGTA) supplemented with thapsigargin (10 µM) and then further incubated in efflux medium, which was collected and replaced every two min for counting in a scintillation counter. Efflux was measured for up to 18 minutes. After 10 min of efflux, IP_3 and A23187 were used as stimuli to trigger $^{45}Ca^{2+}$ mobilization from the ER. Resveratrol or DMSO as vehicle were applied to intact cells or to permeabilized cells during the load phase or efflux phase as indicated in the figures. The Ca^{2+} content of the stores is expressed in counts per minute (cpm), while the Ca^{2+} release was expressed as fractional Ca^{2+} release (% / 2 min), which is the amount of Ca^{2+} released during the 2-min sampling period relative to the Ca^{2+} content at that time.

2.7. Cytotoxicity assay

Cytotoxicity of BAPTA-AM and resveratrol was measured in HeLa cells using the CellTox^{TM} Green assay (Promega, Leiden, The Netherlands). Cells were plated on 96-well plates (Greiner, Vilvoorde, Belgium) and the CellTox^{TM} Green dye was added at a 1:1000 dilution. Subsequently, cells were treated for 2 h with resveratrol (80 µM), BAPTA-AM (10 µM) or the combination of both. DMSO (vehicle) treatment was used as a negative control and lysis solution as a positive control while wells without cells served as a background control. Cytotoxicity was assessed by measuring the fluorescence (485/520 nm excitation/emission) with a FlexStation 3 microplate reader (Molecular Devices). Data were expressed as a percentage of positive control, which was set as 100 %.

2.8. Statistics

All experiments have been repeated at least three independent times. Statistical analysis was performed using one-way ANOVA (non-parametric test) with Bonferroni post hoc test for multiple comparisons.

3. Results

3.1. Resveratrol induces autophagic flux in HeLa cells

By monitoring lipidation of microtubule-associated protein 1 light chain 3 (LC3), we assessed the time-dependent effect of resveratrol (80 µM) on autophagy in HeLa cells. We observed, that already after 1 hour of treatment, resveratrol (80 µM) significantly increased the LC3-II levels (relative to GAPDH) (Fig. 1A). The analysis of all independent experiments is shown in Fig. 1B. To assess whether resveratrol induced autophagic flux or blocked autophagosomal fusion, we determined whether resveratrol was able to induce autophagy in the presence of Bafilomycin A1 (100 nM), added during the last hour of resveratrol treatment (Fig. 1C). The analysis of all independent experiments is shown in Fig. 1D. Resveratrol caused a prominent increase in LC3-II levels (relative to GAPDH) in the presence of Bafilomycin A1, indicating that resveratrol induced an autophagic flux.

3.2. Resveratrol-induced autophagy requires cytosolic Ca^{2+}

As starvation- and rapamycin-induced autophagy is dependent on cytosolic Ca^{2+} [8, 9], we assessed whether resveratrol-induced autophagic flux was dependent on cytosolic Ca^{2+} signaling. Therefore, we determined the effect of BAPTA-AM (10 µM), an intracellular Ca^{2+} chelator, on resveratrol-induced autophagic flux. Fig. 2A shows a representative experiment, while Fig. 2B shows the quantitative analysis of all independent experiments. Here, we focused on the 2 hours resveratrol (80 µM) incubation period, a condition that reliably induced autophagy (Fig. 1). BAPTA-AM was added to the cells for the complete period of resveratrol addition. Strikingly, cells loaded with BAPTA-AM did not display an increase in LC3-II levels in response to resveratrol. Fig. 2B shows that resveratrol-induced autophagy is dependent on the availability of cytosolic Ca^{2+}. A cellular toxicity assay was performed to ascertain that neither the treatment with BAPTA-AM nor the treatment with resveratrol nor their combined treatment was detrimental to the cells. None of the conditions however induced cell toxicity (Supplemental Figure 1).

3.3. Resveratrol-induced autophagy requires the presence of IP_3Rs

As starvation-induced autophagy is dependent on IP_3R activity [8], we assessed the contribution of IP_3R channels in resveratrol-induced autophagic flux. Full pharmacological inhibition of the IP_3R cannot always be achieved [40], while non-specific effects on other Ca^{2+}-handling proteins [41-43] can interfere with the interpretation of the results. Therefore, we here used HEK 3KO cells, a recently established human cell line model (HEK293 cells) in which all three IP_3R isoforms have been knocked out using CRISPR/Cas9 technology [34]. The newly developed HEK 3KO + IP_3R1 cells, in which rat IP_3R1 was functionally reconstituted, were used as an additional control. We first validated the absence or presence of IP_3Rs using an immunoblotting approach that is based on a pan anti-IP_3R antibody, recognizing all three IP_3R isoforms [35]. In contrast to HEK293 wt cells, HEK 3KO cells fully lack IP_3R expression while HEK 3KO + IP_3R1 cells express high levels of IP_3R1 (Supplemental Figure 2). We next assessed the effect of resveratrol (80 µM, 2 hours) on LC3-II-protein levels in HEK293 wt and HEK 3KO cells. All experiments were performed in the presence of Bafilomycin A1 to assess autophagic flux. Fig. 3A shows a representative experiment, while Fig. 3B shows the quantitative analysis of all independent experiments. The immunoblot analysis showed that resveratrol was able to induce a significant increase in LC3-II levels in HEK293 wt cells, but not in HEK 3KO cells. The lack of LC3-II increase in HEK 3KO cells could be overcome by overexpression of IP_3R1 in these cells, as HEK 3KO + IP_3R1 too displayed an increase in LC3-II levels upon resveratrol exposure. We thus show for the first time in a human cell model that IP_3Rs are essential for driving resveratrol-induced autophagic flux.

3.4. Role of Ca^{2+} on upstream elements of resveratrol-activated autophagy pathways

Resveratrol is pleiotropic in its action and can induce autophagy by multiple pathways, including by affecting AMPK, Akt and mTOR activity. To analyze which of these pathways are targeted by resveratrol in HeLa and in HEK cells and which steps could be Ca^{2+}-sensitive, we investigated the phosphorylation levels before and after treatment with resveratrol (80 µM, 2 h) of AMPK, Akt and S6. Phosphorylation of the latter by p70S6K reflects the level of mTOR activity. Neither in HeLa cells (Fig. 4A) nor in HEK cells (Fig. 4B) did resveratrol significantly modulate AMPK and Akt phosphorylation levels. S6 phosphorylation however decreased by over 75% in both cell types indicating

an important inhibition of the mTOR/p70S6K pathway by resveratrol. In HeLa cells, the simultaneous presence of intracellular BAPTA however did not abrogate the ability of resveratrol to inhibit this pathway, as S6 phosphorylation is suppressed by resveratrol in the absence and presence of BATPA-AM. Likewise, resveratrol could inhibit mTOR activity irrespective of the presence of IP_3Rs, as resveratrol decreased S6 phosphorylation in HEK293 wt, the HEK 3KO and the HEK 3KO + IP_3R1 cells (Fig. 4). This indicates that resveratrol inhibits the mTOR/p70S6K pathway and that IP_3Rs and cytosolic Ca^{2+} are dispensable in this process.

3.5. Resveratrol dampens agonist-induced Ca^{2+} release

Resveratrol has been previously proposed to increase by itself cytosolic Ca^{2+} levels [28-30, 44]. However, most of these studies have been based on Fura-2, a ratio-metric Ca^{2+} dye that is not compatible with resveratrol as recent studies indicated that Fura-2 fluorescence is affected by resveratrol, likely independently of changes in $[Ca^{2+}]$ [31-33]. We now investigated the impact of resveratrol concentration ranges known to induce autophagy on basal cytosolic Ca^{2+} levels and on agonist-induced Ca^{2+} release. This was performed, using Fluo-4, a cytosolic Ca^{2+} probe that has a fluorescence profile that is compatible with the fluorescent properties of resveratrol [32]. We acutely added resveratrol in a concentration range of 50 to 100 µM to intact HeLa cells and monitored Fluo-4 fluorescence (Fig. 5A). We found that resveratrol did not provoke a rise in the cytosolic $[Ca^{2+}]$. Using 20 µM ATP as an extracellular agonist, these cells were capable of agonist-induced Ca^{2+} release. Yet, resveratrol dampened this Ca^{2+} response to agonists by about 40% (Fig. 5A, quantitative analysis in Fig. 5B).

3.6. Resveratrol neither mobilizes Ca^{2+} from ER Ca^{2+} stores nor inhibits IP_3R-mediated Ca^{2+} release in permeabilized HeLa cells

To further investigate how resveratrol-induced autophagy depends on Ca^{2+} signaling and IP_3Rs and how agonist-induced Ca^{2+} release was affected by resveratrol, we performed $^{45}Ca^{2+}$-flux assays in permeabilized HeLa cells. This technique allows to gain direct access to the intracellular Ca^{2+} stores and the IP_3R channels (Fig. 6). The ER Ca^{2+} stores were loaded to steady state with $^{45}Ca^{2+}$, after which 10 µM thapsigargin was added to completely block SERCA activity and thus monitor passive $^{45}Ca^{2+}$ leak from the ER in unidirectional flux conditions. Different resveratrol concentrations were applied during the $^{45}Ca^{2+}$-efflux phase. Clearly, in permeabilized cells, resveratrol, up to 80 µM,

a condition known to induce autophagy, did not affect in a direct way the passive Ca^{2+} leak from the ER (Fig. 6A). A23187, a Ca^{2+} ionophore, was used as a positive control to show $^{45}Ca^{2+}$ flux from the ER Ca^{2+} stores.

We also studied the effect of resveratrol on ER $^{45}Ca^{2+}$ uptake, which is mediated by the sarco- and endoplasmic reticulum Ca^{2+} ATPase (SERCA) (Fig. 6B). We therefore monitored $^{45}Ca^{2+}$ uptake in conditions for optimal SERCA activity, including a high ATP concentration (5 mM), in the presence of different resveratrol concentrations. However, resveratrol, up to 80 µM, did not affect ER $^{45}Ca^{2+}$ loading in permeabilized cells, indicating that resveratrol does not affect SERCA activity directly.

We next studied whether resveratrol could directly impact IP_3R-mediated Ca^{2+} release (Fig. 6C). We therefore applied different concentrations of resveratrol from 4 minutes before IP_3 to 4 min after IP_3 addition. Unidirectional Ca^{2+} release was provoked by 0.6 µM IP_3. Resveratrol, up to 80 µM, did not affect in a direct way IP_3-induced Ca^{2+} release in permabilized cells. Additionally, we wanted to determine the long-term effect of resveratrol on intracellular Ca^{2+} mobilization (Fig. 6D). Pre-treatment of HeLa cells for 4 hours with 100 µM resveratrol did also not alter the IP_3-induced Ca^{2+} release elicited in permeabilized cells by two sub-maximal concentrations of IP_3. These results indicate that resveratrol does neither affect directly ER Ca^{2+}-transport systems upon acute exposure nor induce ER Ca^{2+}-store remodeling after long-term exposure.

3.7. Resveratrol depletes the ER Ca^{2+} stores

As none of the Ca^{2+}-transport mechanisms present in the ER seem directly affected by resveratrol, we further investigated whether resveratrol could impact the ER Ca^{2+}-store content in intact cells. Therefore, intraluminal ER Ca^{2+} levels were followed in real time by using the genetically encoded Ca^{2+} indicator G-CEPIA1er [37, 45]. Our results indicate that both in intact HeLa cells (Fig. 7A) and in intact HEK293 wt cells (Fig. 7B), resveratrol at concentrations of 50 µM and 100 µM decreased the Ca^{2+} content of the ER compared to DMSO treatment. Importantly, the ER Ca^{2+} stores of HEK293 wt cells (Fig. 7B) and HEK 3KO cells (Fig. 7C) were equally susceptible to resveratrol exposure, as the decrease in Ca^{2+} content was very similar between HEK293 wt and HEK 3KO cells. This decrease occurring in control conditions (DMSO) or in the presence of resveratrol (50 µM and 100 µM) was quantified for the three cell types by measuring the decrease in normalized G-CEPIA1er fluorescence between t_{70sec} and t_{270sec} (Fig. 7D).

The -ΔF/F0 values for HEK293 wt and HEK 3KO cells were similar. Of note, in this set of experiments, the addition of EGTA partially depleted the ER Ca^{2+} stores in both HEK293 wt and HEK 3KO cells but not in HeLa cells. This likely accounts for the lower -ΔF/F0 values for resveratrol in the HEK cells compared to the HeLa cells. To confirm that resveratrol also decreased ER Ca^{2+} levels in the conditions used to assess agonist-induced Ca^{2+} release, we applied thapsigargin to intact Fluo-4-loaded HeLa cells pretreated with resveratrol (Fig. 8A). The thapsigargin-induced cytosolic [Ca^{2+}] rise was significantly reduced after pre-incubation with 50 or 100 µM resveratrol (Fig. 8B), confirming the decreased ER Ca^{2+} store content.

4. Discussion

The major findings of this study are that resveratrol induces autophagy in an IP_3R/Ca^{2+}-dependent manner while its acute application to cells causes ER Ca^{2+} depletion in an IP_3R-independent manner. As we have previously shown that starvation- and rapamycin-induced autophagy required IP_3R function and cytosolic Ca^{2+} signaling [8, 9], this study therefore indicates that functional IP_3R channels and cytosolic Ca^{2+} signaling likely are of general and fundamental importance for driving autophagic flux.

Resveratrol has been previously implicated in inducing autophagy in a variety of cellular systems. Resveratrol-induced autophagy appears to be at least partially independent of Beclin 1, suggesting the involvement of a non-canonical autophagy pathway [26]. Further work revealed that resveratrol induced autophagy by activating sirtuins [46], which contributed to the longevity effects in animal models like C. elegans [19, 46]. This effect was lost in C. elegans models lacking genes essential for autophagy. Resveratrol has also been shown to be involved in protecting cardiac cells against hypoxia/reoxygenation and ischemia/reperfusion by activating autophagy through regulation of the mTOR complex 2 [47]. Furthermore, resveratrol-induced autophagy has been identified as a cell death-inducing pathway in several cancer cell types, including ovarian cancers [48] and breast cancers [26]. Resveratrol-induced cell death is critically dependent on its ability to induce autophagy [49]. The cell death likely involves caspase-dependent [49] and caspase-independent mechanisms [26]. Besides its autophagy-promoting effects, resveratrol has also been shown to suppress autophagy induced by starvation and rapamycin by targeting and inhibiting p70S6K, a downstream target of the mTOR pathway [20]. In this study, we confirmed that resveratrol by itself is able to rapidly induce autophagy within the first hour of

application, and is at least partially dependent on the inhibition of p70S6K, either directly, or indirectly via impacting mTOR [21].

Resveratrol has also been associated with intracellular Ca^{2+} signaling in several studies [28, 30]. In platelets, resveratrol inhibits thrombin-induced Ca^{2+} influx [50]. In immortalized human mesangial cells, resveratrol inhibits the detrimental Ca^{2+} rise provoked by uric acid [51]. Other studies have suggested that resveratrol could directly cause a rise in cytosolic [Ca^{2+}] [28-30, 44], which was proposed to originate from intracellular Ca^{2+} stores [29]. Resveratrol Ca^{2+}-release properties have been attributed as a major factor for causing mitochondrial depolarization and inducing cell death in breast cancer cells [28]. In prostate cancer cell lines PC3 and DU145, administration of resveratrol decreased ER Ca^{2+} content and inhibited store-operated calcium entry (SOCE), leading to ER stress and autophagy induction [52]. Besides modulating the Ca^{2+} signaling, resveratrol also proved to directly inhibit SOCE by downregulating stromal interaction molecule 1 (STIM1). Decreased STIM1 expression evoked autophagy-dependent cell death [52]. Unfortunately, most Ca^{2+} studies have been based on changes in the fluorescence of the ratiometric Ca^{2+} dye Fura-2 [28-30, 44]. Recently, three independent reports [31-33] provided compelling evidence that resveratrol interferes with Fura-2 fluorescence, independently of changes in [Ca^{2+}]. Resveratrol directly increases the F_{340} excitation / F_{510} emission values without simultaneously decreasing F_{380} excitation / F_{510} emission values due to its intrinsic fluorescent properties. Therefore, we analyzed the effect of resveratrol on intracellular Ca^{2+} dynamics using Fluo-4 and G-CEPIA1er in intact cells and $^{45}Ca^{2+}$ in permeabilized cells. These results demonstrated that although the cytosolic Ca^{2+} levels were not affected in intact cells by resveratrol, and that in permeabilized cells resveratrol did not affect directly any of the ER Ca^{2+}-transport systems (SERCA, IP_3R, Ca^{2+} leak), it rapidly decreased the ER Ca^{2+} content. The lack of cytosolic Ca^{2+} response is in full agreement with previous data from the Roe lab, who showed that resveratrol did not provoke cytosolic [Ca^{2+}] rises in breast cancer cells, either loaded with Fluo-4 or expressing the genetically encoded Ca^{2+} sensor YC3.60 [32]. In spite of the lack of a cytosolic Ca^{2+} response to resveratrol, and of a direct effect of resveratrol on the various ER Ca^{2+}-transport systems, we could clearly demonstrate that Ca^{2+} rapidly disappeared from the ER, underlying the observed dampening of ATP-induced Ca^{2+} release in intact HeLa cells exposed to resveratrol. The mechanism responsible for the decrease in ER Ca^{2+} content in response to resveratrol is probably related to the observation that resveratrol

inhibits the mitochondrial ATP production in intact HeLa cells, leading to a decreased SERCA activity [53] so that a basal Ca^{2+} leak is uncovered. Nevertheless, the lack of a cytosolic Ca^{2+} rise in response to resveratrol is not fully understood, but may involve Ca^{2+} transfer into other organelles and Ca^{2+} rises in microdomains that are insensitive to Fluo-4, which is in the bulk of the cytosol. In addition to this, Ca^{2+} ions may be rapidly buffered and/or can be rapidly pumped out of the cytosol, thereby escaping detection by Fluo-4.

Although resveratrol did not provoke a [Ca^{2+}] increase in the bulk cytosol, its autophagy-inducing effects were dependent on the availability of cytosolic Ca^{2+}, since chelation of intracellular Ca^{2+} could suppress these effects. In line with our studies, Ca^{2+} signaling has also been previously implicated in the autophagy-inducing properties of resveratrol. Indeed, resveratrol has been shown to induce AMPK activation and LC3-II accumulation in A549 human lung adenocarcinoma cells. These effects could be prevented when resveratrol was applied in the presence of extracellular EGTA, a Ca^{2+} chelator, indicating that resveratrol-induced autophagy required extracellular Ca^{2+} [44]. We also found that IP_3Rs must be present for driving resveratrol-induced autophagy, as cells devoid of IP_3R expression did not display resveratrol-induced autophagy. Thus, despite the fact that resveratrol can on the short-term deplete the ER Ca^{2+} stores in the absence of IP_3Rs, resveratrol still requires IP_3Rs and Ca^{2+} signaling to induce on the long-term autophagic flux. This shows that the ER Ca^{2+} leak uncovered by resveratrol is not sufficient *per se* to induce autophagy, as resveratrol provokes ER Ca^{2+} depletion in both IP_3R-expressing and IP_3R-deficient cells, but only induces autophagic flux in IP_3R-expressing cells. The role of IP_3Rs and cytosolic Ca^{2+} in resveratrol-induced autophagy could also not be attributed to alterations in mTOR activity, since the inhibition of S6 phosphorylation by resveratrol was not abrogated by buffering intracellular Ca^{2+} or by IP_3R knockout.

This puts IP_3Rs and ER-originating Ca^{2+}-release events at the center for upregulating autophagic flux, not only in canonical mTOR-dependent autophagy but also in non-canonical autophagy pathways. The unique contribution of IP_3Rs to resveratrol-induced autophagic flux requires further examination. In particular, IP_3Rs may serve as a recruitment platform for pro-autophagic proteins, thereby playing an essential role in driving autophagy. This property may be independent of its Ca^{2+} signaling function, as obviously resveratrol depletes the ER of Ca^{2+} independently of IP_3Rs while resveratrol-induced autophagy is strictly dependent on IP_3Rs. Alternatively, IP_3Rs may reside in

certain ER microdomains, which are differentially affected by resveratrol than the “bulk” ER, whereby part of their Ca^{2+}-signaling function remains operational and contributes to driving autophagic flux, *e.g.* in conjunction with the Ca^{2+}-handling properties of the lysosomes [54-56]. It is also interesting to note that resveratrol appears to act differently than other Ca^{2+}-modulating agents like Ca^{2+} ionophore or the SERCA inhibitor thapsigargin, which have been implicated in blocking autophagosome formation [57].

To conclude, we show that autophagy induction by natural compounds like resveratrol that likely act in part via mTOR-independent pathways is critically dependent on cytosolic Ca^{2+} signaling and IP_3R presence/function. Thus, IP_3Rs and Ca^{2+} signaling appear to be an integral part of the cellular responses needed for increasing autophagic flux in response to cellular stress and natural compounds, like resveratrol.

Acknowledgments

We thank Anja Florizoone and Marina Crabbé for technical support. GR and MB are recipients of Ph.D. fellowships of the Research Foundation—Flanders (FWO). This work was supported by the Interuniversity Attraction Poles Program (Belgian Science Policy) P7/13 and by FWO grant G.0634.13N to JBP and GB. DIY, JBP and GB are part of the FWO Scientific Research Community CaSign (W0.019.17N).

References

1. Bento, C.F., et al., *Mammalian autophagy: How does it work?* Annu Rev Biochem, 2016. **85**: p. 685-713.
2. Levine, B. and G. Kroemer, *Autophagy in the pathogenesis of disease.* Cell, 2008. **132**(1): p. 27-42.
3. Decuypere, J.P., G. Bultynck, and J.B. Parys, *A dual role for Ca^{2+} in autophagy regulation.* Cell Calcium, 2011. **50**(3): p. 242-50.
4. Cardenas, C. and J.K. Foskett, *Mitochondrial Ca^{2+} signals in autophagy.* Cell Calcium, 2012. **52**(1): p. 44-51.
5. Parys, J.B., J.P. Decuypere, and G. Bultynck, *Role of the inositol 1,4,5-trisphosphate receptor/Ca^{2+}-release channel in autophagy.* Cell Commun Signal, 2012. **10**(1): p. 17.
6. Decuypere, J.P., J.B. Parys, and G. Bultynck, *ITPRs/inositol 1,4,5-trisphosphate receptors in autophagy: From enemy to ally.* Autophagy, 2015. **11**(10): p. 1944-8.
7. Ghislat, G., et al., *Withdrawal of essential amino acids increases autophagy by a pathway involving Ca^{2+}/calmodulin-dependent kinase kinase-β (CaMKK-β).* J Biol Chem, 2012. **287**(46): p. 38625-36.
8. Decuypere, J.P., et al., *Ins(1,4,5)P_3 receptor-mediated Ca^{2+} signaling and autophagy induction are interrelated.* Autophagy, 2011. **7**(12): p. 1472-89.
9. Decuypere, J.P., et al., *mTOR-Controlled autophagy requires intracellular Ca^{2+} signaling.* PLoS One, 2013. **8**(4): p. e61020.
10. Kakoti, B.B., et al., *Resveratrol and omega-3 fatty acid: its implications in cardiovascular diseases.* Front Cardiovasc Med, 2015. **2**:38.
11. Bonnefont-Rousselot, D., *Resveratrol and cardiovascular diseases.* Nutrients, 2016. **8:**250.
12. Rege, S.D., et al., *Neuroprotective effects of resveratrol in Alzheimer disease pathology.* Front Aging Neurosci, 2014. **6**:218.
13. Tellone, E., et al., *Resveratrol: A focus on several neurodegenerative diseases.* Oxid Med Cell Longev, 2015. **2015**:392169.
14. Pavan, A.R., et al., *Unraveling the anticancer effect of curcumin and resveratrol.* Nutrients, 2016. **8**:628.
15. Kotecha, R., A. Takami, and J.L. Espinoza, *Dietary phytochemicals and cancer chemoprevention: a review of the clinical evidence.* Oncotarget, 2016. **7**(32): p. 52517-52529.

16. Kulkarni, S.S. and C. Canto, *The molecular targets of resveratrol.* Biochim Biophys Acta, 2015. **1852**(6): p. 1114-23.
17. Borriello, A., et al., *Resveratrol: from basic studies to bedside.* Cancer Treat Res, 2014. **159**: p. 167-84.
18. Howitz, K.T., et al., *Small molecule activators of sirtuins extend Saccharomyces cerevisiae lifespan.* Nature, 2003. **425**(6954): p. 191-6.
19. Morselli, E., et al., *Caloric restriction and resveratrol promote longevity through the Sirtuin-1-dependent induction of autophagy.* Cell Death Dis, 2010. **1**: p. e10.
20. Armour, S.M., et al., *Inhibition of mammalian S6 kinase by resveratrol suppresses autophagy.* Aging (Albany NY), 2009. **1**(6): p. 515-28.
21. Park, D., et al., *Resveratrol induces autophagy by directly inhibiting mTOR through ATP competition.* Sci Rep, 2016. **6**:21772.
22. Frojdo, S., et al., *Resveratrol is a class IA phosphoinositide 3-kinase inhibitor.* Biochem J, 2007. **406**(3): p. 511-8.
23. Vingtdeux, V., et al., *AMP-activated protein kinase signaling activation by resveratrol modulates amyloid-beta peptide metabolism.* J Biol Chem, 2010. **285**(12): p. 9100-13.
24. Ding, D.F., et al., *Resveratrol attenuates renal hypertrophy in early-stage diabetes by activating AMPK.* Am J Nephrol, 2010. **31**(4): p. 363-74.
25. Puissant, A., et al., *Resveratrol promotes autophagic cell death in chronic myelogenous leukemia cells via JNK-mediated p62/SQSTM1 expression and AMPK activation.* Cancer Res, 2010. **70**(3): p. 1042-52.
26. Scarlatti, F., et al., *Role of non-canonical Beclin 1-independent autophagy in cell death induced by resveratrol in human breast cancer cells.* Cell Death Differ, 2008. **15**(8): p. 1318-29.
27. Mauthe, M., et al., *Resveratrol-mediated autophagy requires WIPI-1-regulated LC3 lipidation in the absence of induced phagophore formation.* Autophagy, 2011. **7**(12): p. 1448-61.
28. Sareen, D., et al., *Mitochondria, calcium, and calpain are key mediators of resveratrol-induced apoptosis in breast cancer.* Mol Pharmacol, 2007. **72**(6): p. 1466-75.
29. Garcia-Sanchez, L., *Resveratrol mobilizes Ca^{2+} from intracellular stores and induces c-Jun N-terminal kinase activation in tumoral AR42J cells.* Mol Cell Biochem, 2012. **362**(1-2): p. 15-23.

30. Chang, H.J., et al., *Mechanisms of resveratrol-induced changes in cytosolic free calcium ion concentrations and cell viability in OC2 human oral cancer cells.* Hum Exp Toxicol, 2015. **34**(3): p. 289-99.
31. Paudel, R.C., et al., *Resveratrol is not compatible with a fura-2-based assay for measuring intracellular Ca^{2+} signaling.* Biochem Biophys Res Commun, 2014. **450**(4): p. 1626-30.
32. Kopp, R.F., C.A. Leech, and M.W. Roe, *Resveratrol interferes with fura-2 intracellular calcium measurements.* J Fluoresc, 2014. **24**(2): p. 279-84.
33. Santofimia-Castano, P., G.M. Salido, and A. Gonzalez, *Interferences of resveratrol with fura-2-derived fluorescence in intracellular free-Ca^{2+} concentration determinations.* Cytotechnology, 2016. **68**(4): p. 1369-80.
34. Alzayady, K.J., et al., *Defining the stoichiometry of inositol 1,4,5-trisphosphate binding required to initiate Ca^{2+} release.* Sci Signal, 2016. **9**(422): p. ra35.
35. Bultynck, G., et al., *Thimerosal stimulates Ca^{2+} flux through inositol 1,4,5-trisphosphate receptor type 1, but not type 3, via modulation of an isoform-specific Ca^{2+}-dependent intramolecular interaction.* Bioche J, 2004. **381**(Pt 1): p. 87-96.
36. Vervliet, T., et al., *Ryanodine receptors are targeted by anti-apoptotic Bcl-XL involving its BH4 domain and Lys87 from its BH3 domain.* Sci Rep, 2015. **5**:9641.
37. Bittremieux, M., et al., *DPB162-AE, an inhibitor of store-operated Ca^{2+} entry, can deplete the endoplasmic reticulum Ca^{2+} store.* Cell Calcium, 2017. In press.
38. Missiaen, L., et al., *Ca^{2+} release induced by inositol 1,4,5-trisphosphate is a steady-state phenomenon controlled by luminal Ca^{2+} in permeabilized cells.* Nature, 1992. **357**(6379): p. 599-602.
39. Luyten, T., et al., *Measurement of intracellular Ca^{2+} release in permeabilized cells using $^{45}Ca^{2+}$.* Cold Spring Harb Protoc, 2014. **2014**(3): p. 289-94.
40. Saleem, H., et al., *Interactions of antagonists with subtypes of inositol 1,4,5-trisphosphate (IP_3) receptor.* Br J Pharmacol, 2014. **171**(13): p. 3298-312.
41. De Smet, P., et al., *Xestospongin C is an equally potent inhibitor of the inositol 1,4,5-trisphosphate receptor and the endoplasmic-reticulum Ca^{2+} pumps.* Cell Calcium, 1999. **26**(1-2): p. 9-13.
42. Missiaen, L., et al., *2-Aminoethoxydiphenyl borate affects the inositol 1,4,5-trisphosphate receptor, the intracellular Ca^{2+} pump and the non-specific Ca^{2+}*

leak from the non-mitochondrial Ca^{2+} stores in permeabilized A7r5 cells. Cell Calcium, 2001. **29**(2): p. 111-6.

43. Bootman, M.D., et al., *2-aminoethoxydiphenyl borate (2-APB) is a reliable blocker of store-operated Ca^{2+} entry but an inconsistent inhibitor of $InsP_3$-induced Ca^{2+} release.* FASEB J, 2002. **16**(10): p. 1145-50.
44. Zhang, J., et al., *Autophagic cell death induced by resveratrol depends on the Ca^{2+}/AMPK/mTOR pathway in A549 cells.* Biochem Pharmacol, 2013. **86**(2): p. 317-28.
45. Suzuki, J., et al., *Imaging intraorganellar Ca^{2+} at subcellular resolution using CEPIA.* Nature communications, 2014. **5**: p. 4153.
46. Morselli, E., et al., *The life span-prolonging effect of sirtuin-1 is mediated by autophagy.* Autophagy, 2010. **6**(1): p. 186-8.
47. Gurusamy, N., et al., *Cardioprotection by resveratrol: a novel mechanism via autophagy involving the mTORC2 pathway.* Cardiovasc Res, 2010. **86**(1): p. 103-12.
48. Opipari, A.W., Jr., et al., *Resveratrol-induced autophagocytosis in ovarian cancer cells.* Cancer Res, 2004. **64**(2): p. 696-703.
49. Trincheri, N.F., et al., *Resveratrol-induced apoptosis depends on the lipid kinase activity of Vps34 and on the formation of autophagolysosomes.* Carcinogenesis, 2008. **29**(2): p. 381-9.
50. Dobrydneva, Y., R.L. Williams, and P.F. Blackmore, *Trans-resveratrol inhibits calcium influx in thrombin-stimulated human platelets.* Br J Pharmacol, 1999. **128**(1): p. 149-57.
51. Albertoni, G. and N. Schor, *Resveratrol inhibits the intracellular calcium increase and angiotensin/endothelin system activation induced by soluble uric acid in mesangial cells.* Braz J Med Biol Res, 2015. **48**(1): p. 51-56.
52. Selvaraj, S., et al., *Resveratrol activates autophagic cell death in prostate cancer cells via downregulation of STIM1 and the mTOR pathway.* Mol Carcinog, 2016. **55**(5): p. 818-31.
53. Madreiter-Sokolowski, C.T., et al., *Resveratrol specifically kills cancer cells by a devastating increase in the Ca^{2+} coupling between the greatly tethered endoplasmic reticulum and mitochondria.* Cell Physiol Biochem, 2016. **39**(4): p. 1404-20.

54. Kilpatrick, B.S., et al., *Direct mobilisation of lysosomal Ca^{2+} triggers complex Ca^{2+} signals.* J Cell Sci, 2013. **126**(Pt 1): p. 60-6.

55. Morgan, A.J., et al., *Bidirectional Ca^{2+} signaling occurs between the endoplasmic reticulum and acidic organelles.* J Cell Biol, 2013. **200**(6): p. 789-805.

56. Lopez-Sanjurjo, C.I., et al., *Lysosomes shape Ins(1,4,5)P_3-evoked Ca^{2+} signals by selectively sequestering Ca^{2+} released from the endoplasmic reticulum.* J Cell Sci, 2013. **126**(Pt 1): p. 289-300.

57. Engedal, N., et al., *Modulation of intracellular calcium homeostasis blocks autophagosome formation.* Autophagy, 2013. **9**(10): p. 1475-90.

Figure legends

Fig. 1. Resveratrol induces autophagic flux in HeLa cells. (A) A representative blot showing LC3-II and GAPDH-protein levels from lysates obtained from untreated (control), DMSO-treated (vehicle) and resveratrol-treated (80 µM) HeLa cells for 1 to 6 hours. (B) Quantification of LC3-II/GAPDH levels from four independent experiments relative to the control, which was set as 1. Mean values ± S.D. are presented; * indicates a significant difference with the control ($P<0.05$). (C) A representative blot showing LC3-II and GAPDH-protein levels from lysates obtained from untreated (control), DMSO-treated (vehicle) and resveratrol-treated (80 µM) HeLa cells for 1 to 6 hours in the presence of Bafilomycin A1 (100 nM, added during the last hour). (D) Quantification of LC3-II/GAPDH levels from seven independent experiments relative to the control, which was set as 1. Mean values ± S.D. are presented; * and ** indicates a significant difference with the control ($P<0.05$ and $P<0.01$, resp.).

Fig. 2. Resveratrol-induced autophagy requires cytosolic Ca^{2+}. (A) A representative blot showing LC3-II and GAPDH-protein levels from lysates obtained from HeLa cells treated with DMSO (vehicle) or treated with resveratrol (80 µM) for 2 hours in the presence of Bafilomycin A1 (100 nM) and in the absence or presence of BAPTA-AM (10 µM). (B) Quantification of LC3-II/GAPDH levels of the different experiments performed relative to the control, which was set as 1. Mean values ± S.D. are presented, N = 10; * indicates a significant difference with the control ($P<0.05$). $ indicates a significant difference with the resveratrol + BAPTA-AM condition ($P<0.05$).

Fig. 3. Resveratrol-induced autophagy requires the presence of IP_3Rs. (A) A representative blot showing LC3-II and GAPDH-protein levels from lysates obtained from HEK293 wt cells and HEK 3KO cells, untreated (control), treated with DMSO (vehicle), or treated with resveratrol (80 µM) for 2 hours in the presence of Bafilomycin A1 (100 nM). (B) Quantification of LC3-II/GAPDH levels of the different experiments performed relative to the control, which was set as 1. Mean values ± S.D. are presented, N = 14; * and *** indicate a significant difference compared to control ($P<0.05$ and $P<0.001$, respectively), while # and ## indicate a significant difference compared to vehicle ($P<0.05$ and $P<0.01$, respectively).

Fig. 4. Resveratrol reduces phospho-S6 levels, but neither phospho-AMPK nor phospho-Akt levels, independently of the availability of cytosolic Ca^{2+} or of the presence of IP_3Rs. (A) Representative blots showing phospho-AMPK and total AMPK, phospho-Akt and total Akt and phospho-S6 and total S6 in lysates from HeLa cells treated for 2 hours with DMSO (vehicle) or with resveratrol (80 µM) in the absence or presence of BAPTA-AM (10 µM). All cells were exposed to 100 nM Bafilomycin A1 for 2 hours. The immunoreactive signal for both the phosphorylated protein and total protein were always obtained from exactly the same sample loaded on parallel gels. The immunoreactive signals were quantified as the ratio of the phosphorylated/total protein and normalized to 1 for the vehicle control. The mean and S.D. values are presented for each pair of blots (N = 10). ** indicates a significant difference with the control (P<0.01). $$ indicates a significant difference with the resveratrol + BAPTA-AM condition (P<0.01). (B) Representative blots showing phospho-AMPK and total AMPK, phospho-Akt and total Akt and phospho-S6 and total S6 in lysates from HEK293 wt, HEK 3KO cells and HEK 3KO + IP_3R1 in following conditions: untreated (control), treated with DMSO (vehicle) or treated with resveratrol (80 µM) for 2 hours. All cells were exposed to 100 nM Bafilomycin A1 for 2 hours. The immunoreactive signal for both the phosphorylated protein and total protein were always obtained from exactly the same sample loaded on parallel gels. The immunoreactive signals were quantified as the ratio of the phosphorylated/total protein and normalized to 1 for the untreated control. The mean and S.D. values are presented for each pair of blots (N = 15 for HEK293 wt, N = 14 for HEK 3KO and N = 8 for HEK 3KO + IP_3R1). ** indicates a significant difference with the untreated control (P<0.01). ## indicates a significant difference with the vehicle control (P<0.01).

Fig. 5. Resveratrol does not evoke Ca^{2+} signals in the cytosol of HeLa cells, but suppresses agonist-induced Ca^{2+} release. (A) A representative experiment showing the Fluo-4 fluorescence ($F_{ex488/em530}$) in relative fluorescence units (RFU) as a function of time. The addition of 3 mM EGTA (after 30 sec), DMSO or resveratrol (after 70 sec) and 20 µM ATP (after 300 sec) is shown. (B) Quantification of the peak amplitude of the ATP-induced cytosolic Ca^{2+} rise is presented as ΔRFU values, which were calculated as the difference between the peak RFU value and the RFU value just before the addition of ATP and displayed as mean ± S.D. (N = 9). *** and **** indicates a significant difference with the vehicle condition (P<0.001 and P<0.0001, respectively).

Fig. 6. Resveratrol does not affect ER Ca^{2+}-transport systems in plasma membrane-permeabilized HeLa cells. In panel A, C and D, $^{45}Ca^{2+}$ release, calculated as the fractional loss (%) / 2 min, is plotted as a function of time. In panel B, the amount of $^{45}Ca^{2+}$ in the stores, presented in count per minutes (cpm) values, is plotted as a function of time. In case that resveratrol was added during the experiment, the incubation time is indicated with a gray box. Otherwise, cells were pre-treated with resveratrol. The addition of a stimulus (IP_3 or A23187) is indicated with an arrow. All data points represent the mean of two technical replicates ± S.D. All experiments have been independently repeated at least three times. (A) The ER Ca^{2+} stores from permeabilized HeLa cells were loaded with $^{45}Ca^{2+}$ in the presence of ATP until steady state. Efflux was initiated in a medium containing EGTA (1 mM) and thapsigargin (10 µM). During the passive $^{45}Ca^{2+}$ efflux phase resveratrol was added at the indicated concentrations for 8 min. DMSO was applied in the vehicle-exposed samples. A23187, a Ca^{2+} ionophore, was applied as a positive control. A typical experiment is shown. (B) A typical experiment showing the effect of different resveratrol concentrations, added during the complete course of the $^{45}Ca^{2+}$-uptake phase, on total ER $^{45}Ca^{2+}$ uptake. DMSO was applied in the vehicle-exposed samples. (C) A typical experiment showing the acute effect of different resveratrol concentrations on IP_3-induced Ca^{2+} release. Resveratrol was added for 8 minutes, from 4 min before to 4 min after IP_3 addition. Ca^{2+} release through IP_3Rs was triggered by 0.6 µM IP_3. A23187 was added to estimate the total releasable $^{45}Ca^{2+}$. (D) A typical experiment showing the effect of a prolonged incubation of the cells with 100 µM resveratrol for 4 hours, a condition associated with increased autophagy, on IP_3- and A23187-induced Ca^{2+} release. Two concentrations of IP_3 (1 and 3 µM) were assessed.

Fig. 7. Resveratrol provokes ER Ca^{2+} depletion independently of IP_3Rs. ER Ca^{2+} levels were monitored using G-CEPIA1er ($F_{ex488/em530}$) in HeLa (A), HEK293 wt (B) and HEK 3KO (C) single cells. (A-C) Each graph represents a representative experiment showing the normalized mean G-CEPIA1er fluorescence (F/F0) of 12-26 cells as a function of time in HeLa cells (A), HEK293 wt cells (B) or HEK 3KO cells (C). After 30 sec, extracellular Ca^{2+} was chelated by the addition of EGTA (3 mM final concentration). After 70 sec, vehicle (black curves), 50 µM resveratrol (green curves) or 100 µM resveratrol (red curves) was added (final concentrations). After 270 sec, thapsigargin (2

μM final concentration) was added to provoke ER Ca^{2+} depletion by inhibiting SERCA activity. The number of individual cells measured is indicated for each condition. (D) The quantification of the ER Ca^{2+} leak induced by DMSO as vehicle, 50 μM resveratrol or 100 μM resveratrol is presented as $-\Delta F/F0$, which was calculated as -(F/F0 at t_{270sec} – F/F0 at t_{70sec}), where F/F0 at 70 sec represents the normalized fluorescence just before the addition of DMSO and F/F0 at 270sec represents the normalized fluorescence just before the addition of thapsigargin. Data points represent mean ± S.D. (N = 2-3). **** indicates a significant difference compared to vehicle (P<0.0001).

Fig. 8. Resveratrol reduces the amount of thapsigargin-releasable Ca^{2+}. (A) A representative experiment showing the Fluo-4 fluorescence ($F_{ex488/em530}$) in relative fluorescence units (RFU) as a function of time. The addition of 3 mM EGTA (after 30 sec), DMSO or resveratrol (after 70 sec) and 2 μM thapsigargin (after 300 sec) is shown. (B) Quantification of the peak amplitude of the thapsigargin-induced cytosolic Ca^{2+} rise is presented as ΔRFU values, which were calculated as the difference between the peak RFU value and the RFU value just before the addition of ATP and displayed as mean ± S.D. (N = 36). **** indicates a significant difference with the vehicle condition (P<0.0001).

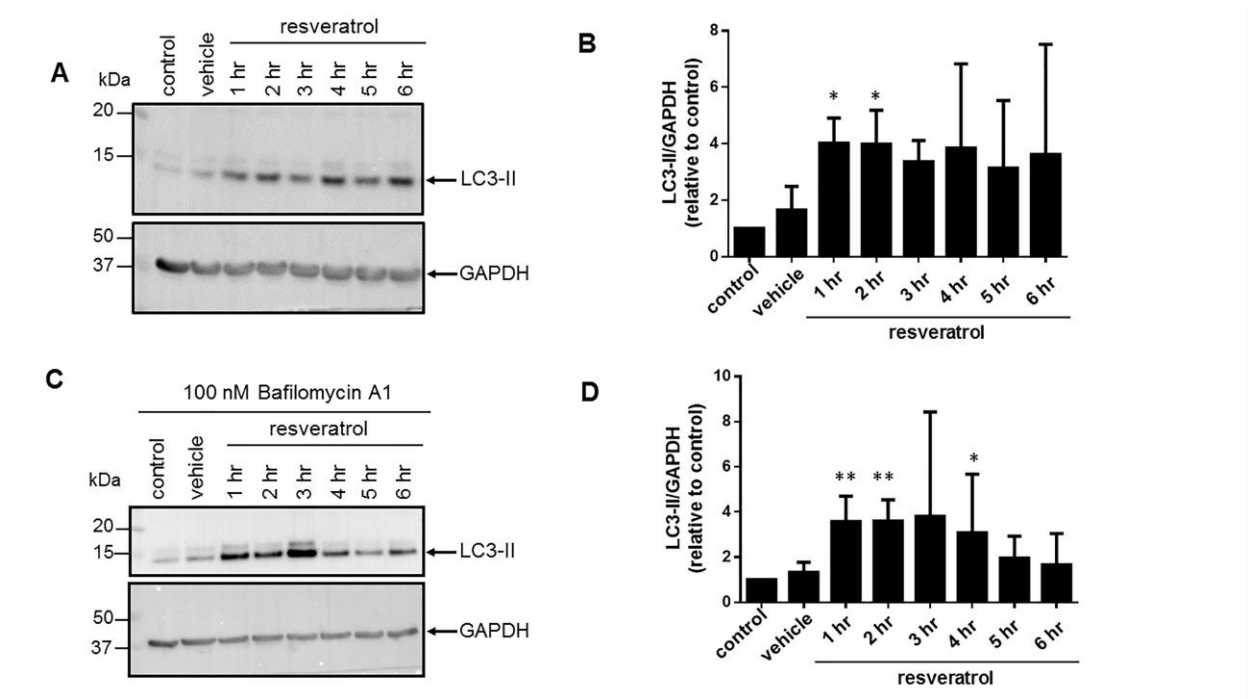

Figure 1

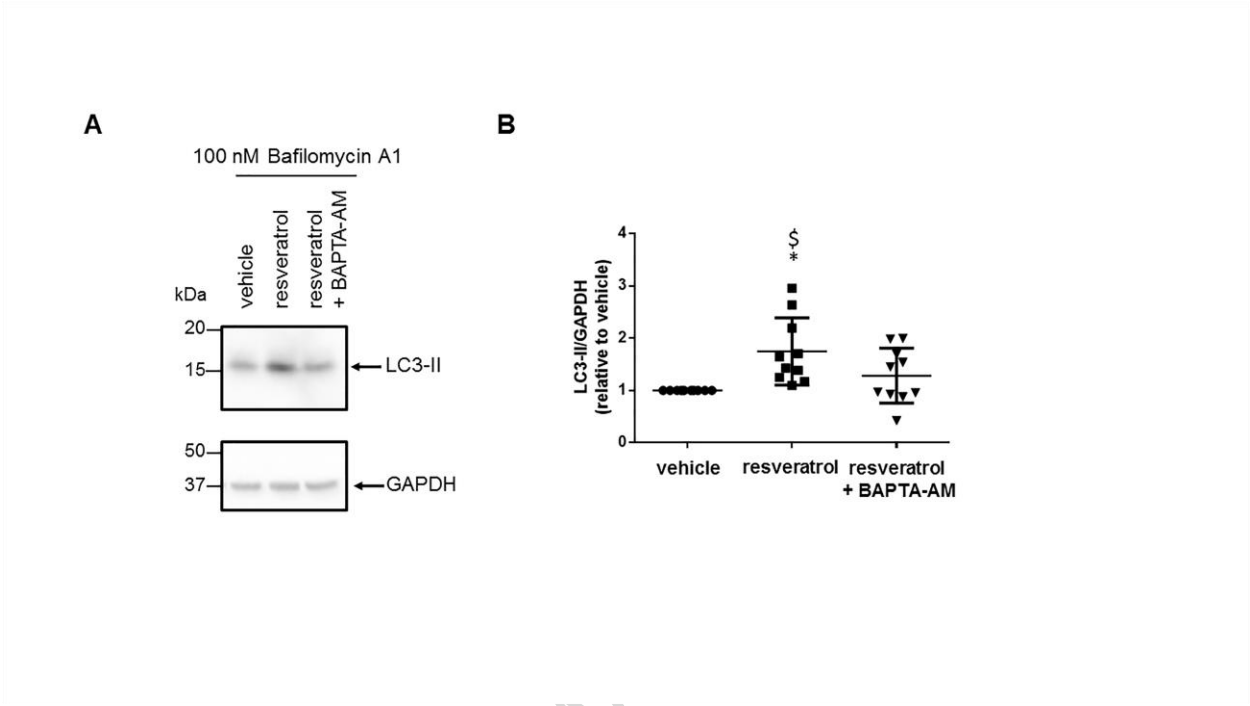

Figure 2

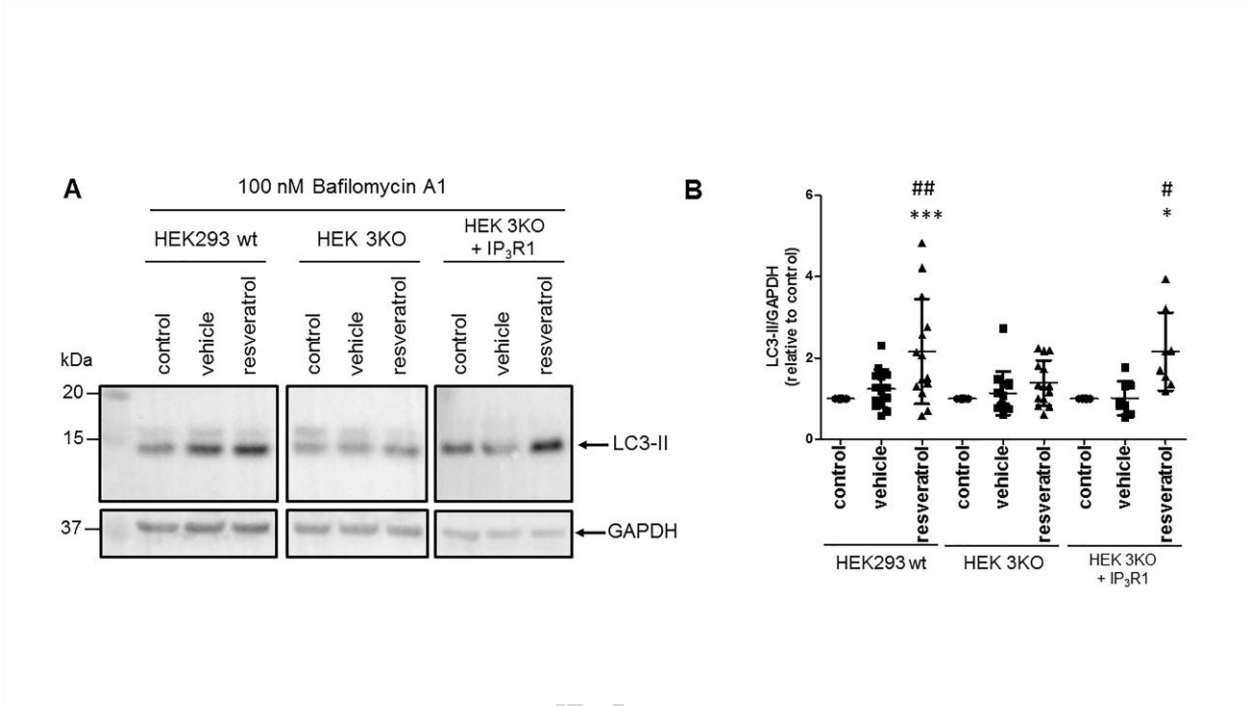

Figure 3

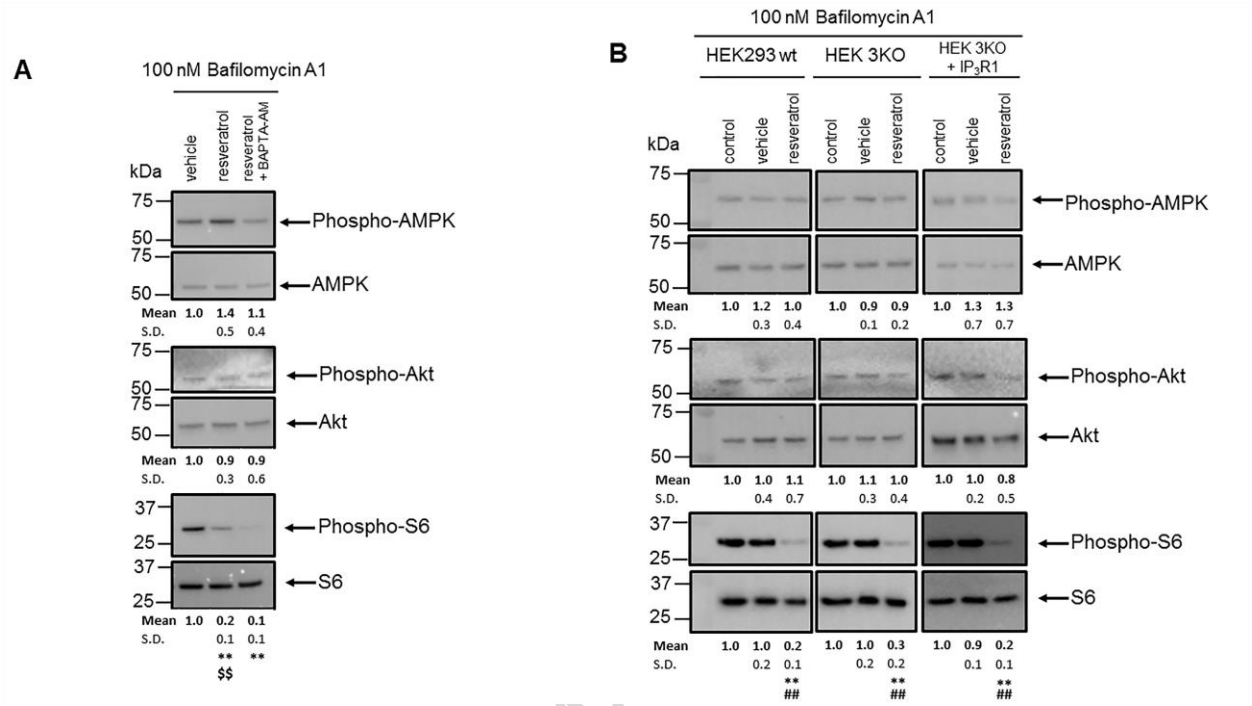

Figure 4

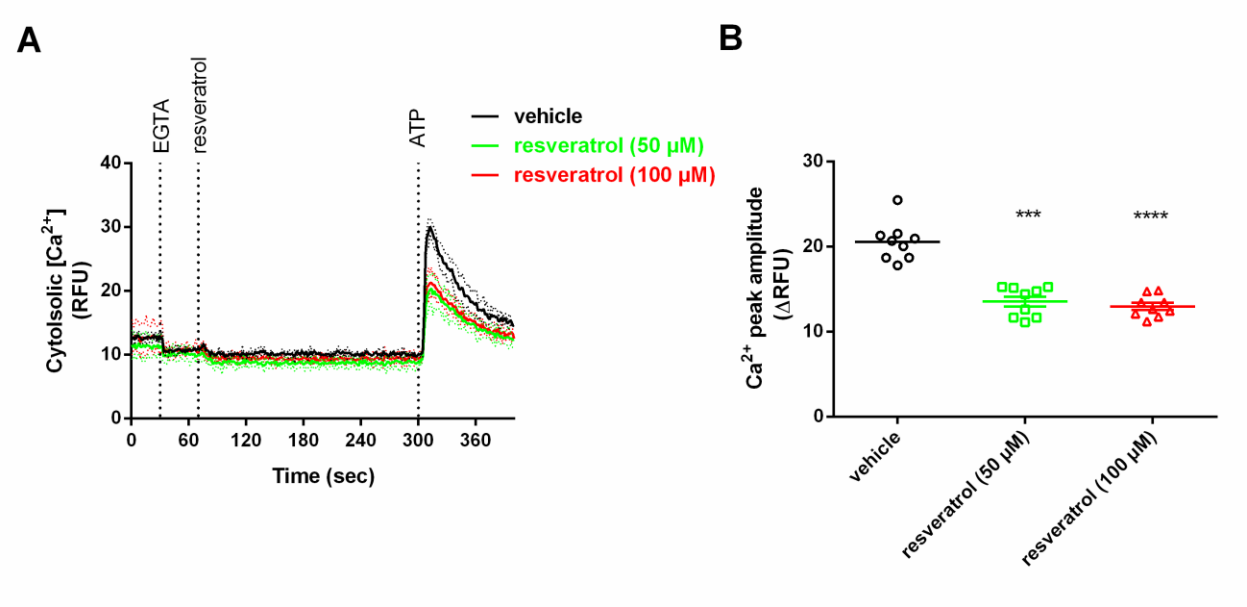

Figure 5

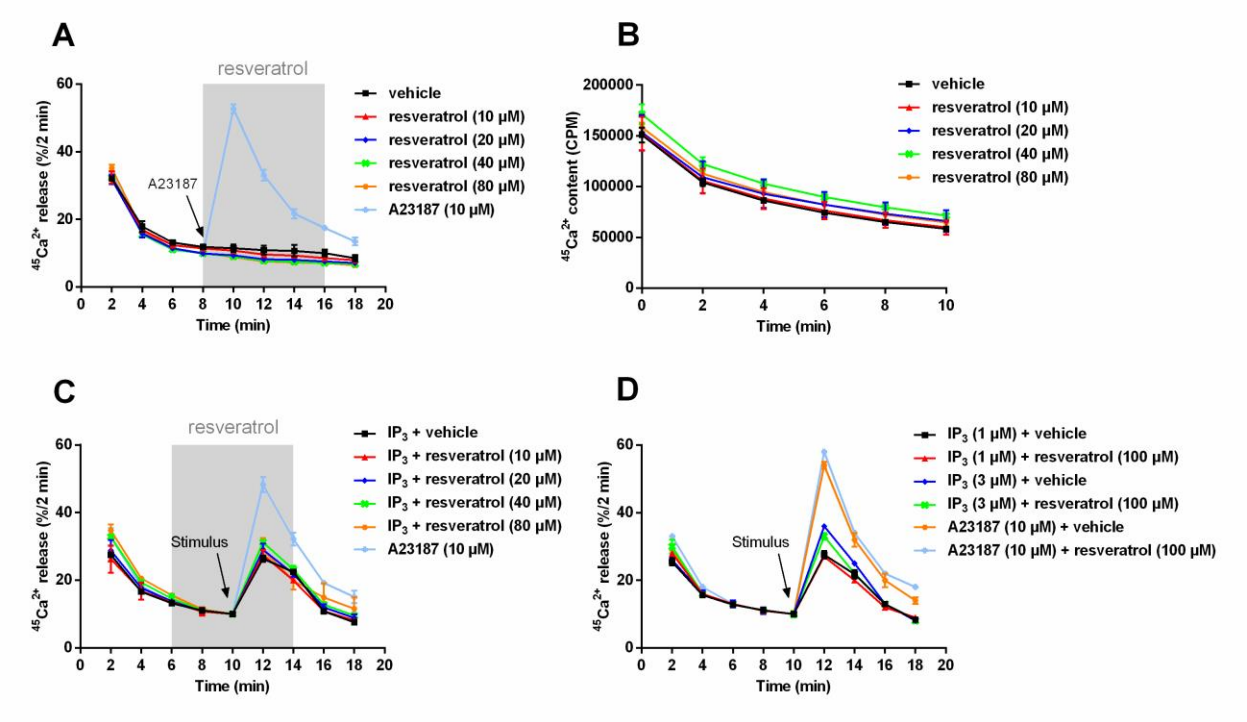

Figure 6

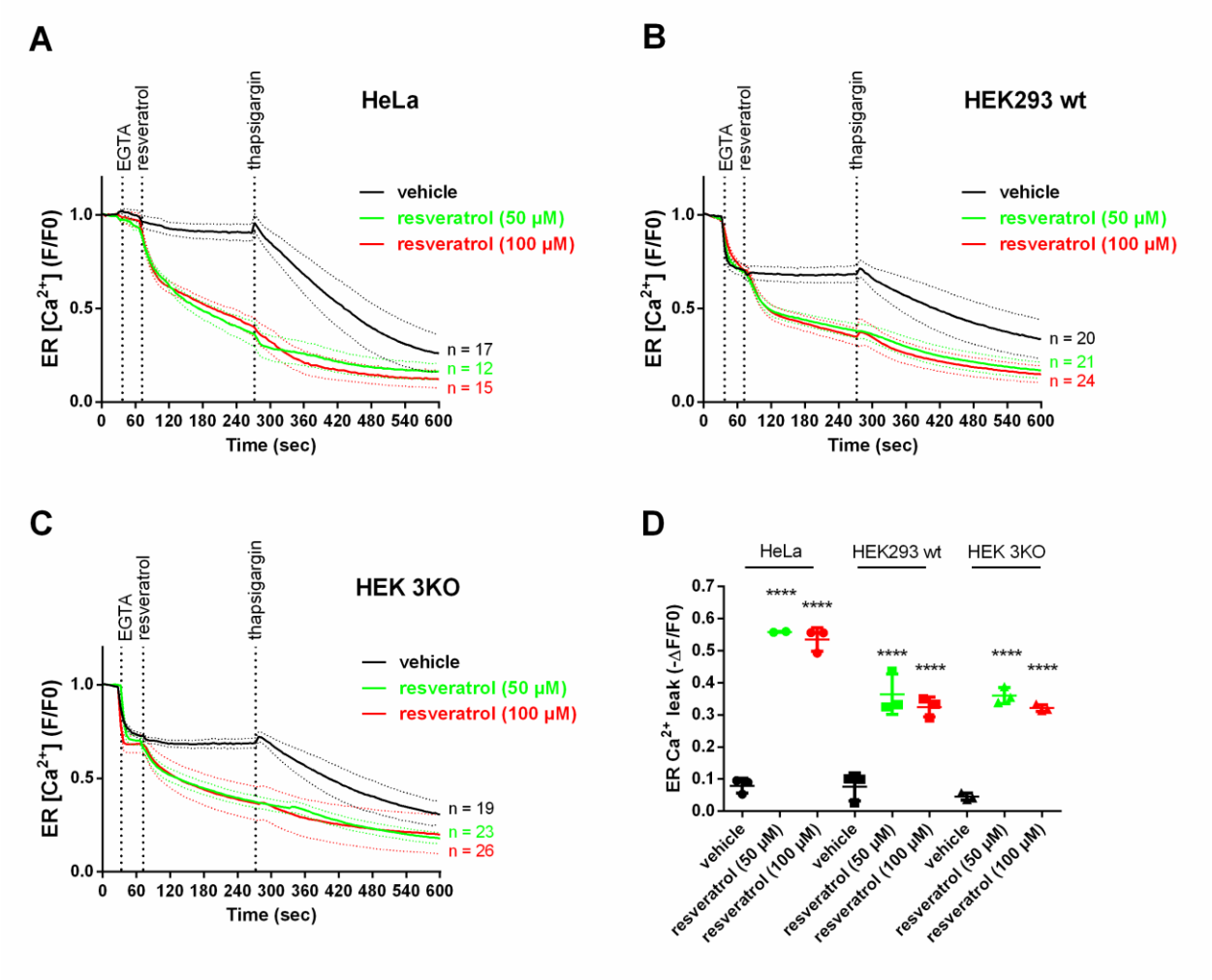

Figure 7

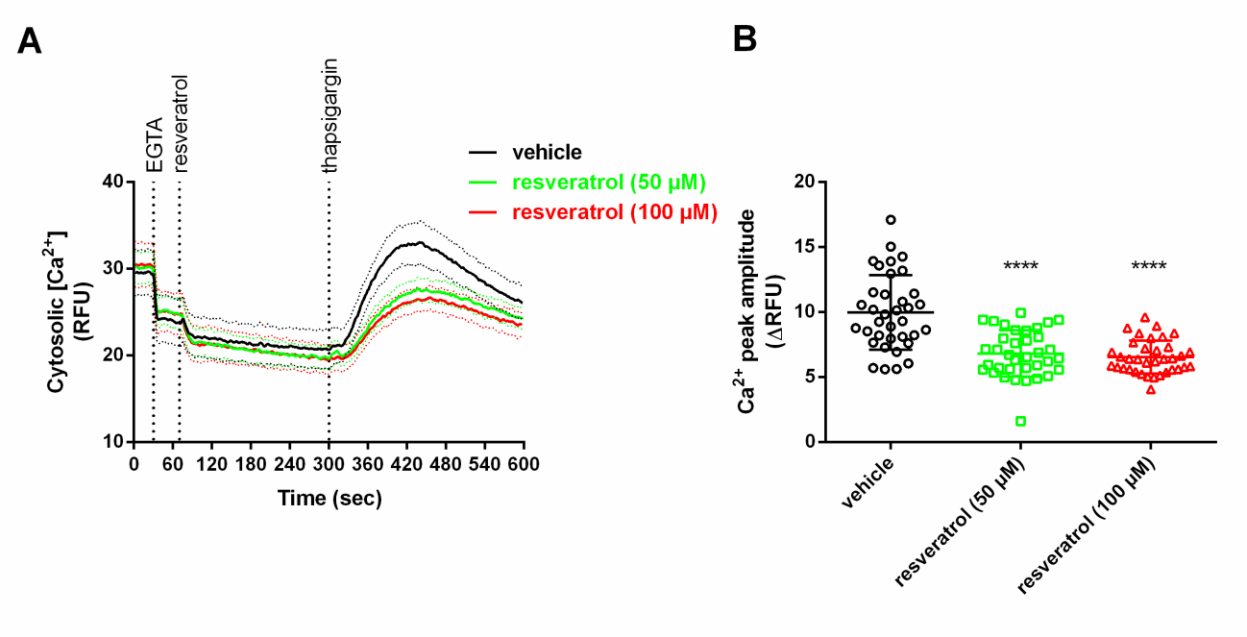

Figure 8

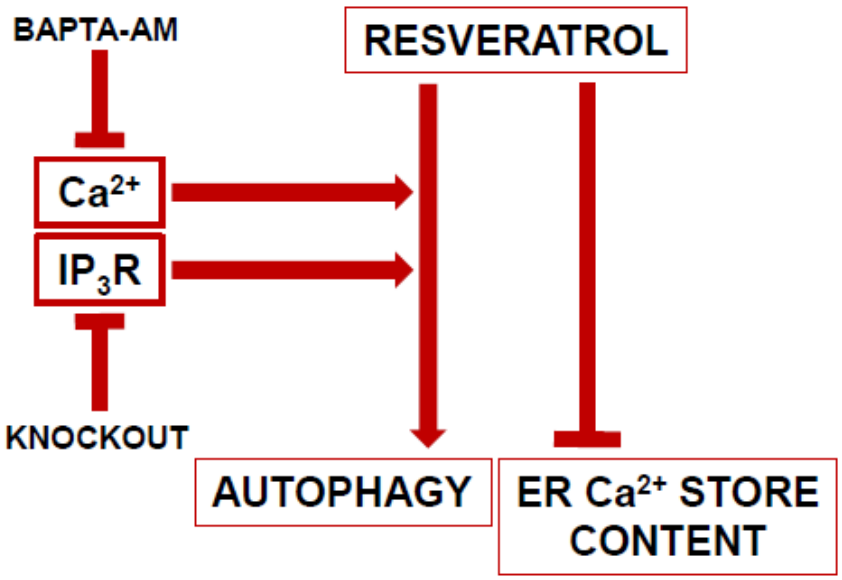

Graphical abstract

Highlights

- Resveratrol rapidly increases autophagic flux
- Resveratrol-induced autophagy depends on cytosolic Ca^{2+} signals
- IP_3 receptors are essential for driving resveratrol-induced autophagy
- Resveratrol decreases ER Ca^{2+} levels independently of IP_3Rs
- The decreased ER Ca^{2+} store content dampens agonist-induced Ca^{2+} release